© 2017. Published by The Company of Biologists Ltd | Development (2017) 144, 2570-2583 doi:10.1242/dev.148171

Synergism between *canoe* and *scribble* mutations causes tumor-like overgrowth via Ras activation in neural stem cells and epithelia

Noemí Rives-Quinto*, Maribel Franco‡, Ana de Torres-Jurado‡ and Ana Carmena§

ABSTRACT

Over the past decade an intriguing connection between asymmetric cell division, stem cells and tumorigenesis has emerged. Neuroblasts, which are the neural stem cells of the *Drosophila* central nervous system, divide asymmetrically and constitute an excellent paradigm for investigating this connection further. Here we show that the simultaneous loss of the asymmetric cell division regulators Canoe (afadin in mammals) and Scribble in neuroblast clones leads to tumor-like overgrowth through both a severe disruption of the asymmetric cell division process and *canoe* loss-mediated Ras-PI3K-Akt activation. Moreover, *canoe* loss also interacts synergistically with *scribble* loss to promote overgrowth in epithelial tissues, here just by activating the Ras-Raf-MAPK pathway. *discs large 1* and *lethal (2) giant larvae*, which are functionally related to *scribble*, contribute to repress the Ras-MAPK signaling cascade in epithelia. Hence, our work uncovers novel cooperative interactions between all these well-conserved tumor suppressors that ensure tight regulation of the Ras signaling pathway.

KEY WORDS: Canoe, Afadin, Scribble, Ras signaling, Tumorigenesis, *Drosophila*

INTRODUCTION

A direct link between defects in the process of asymmetric cell division (ACD) and tumorigenesis was demonstrated for the first time in the neural stem cells of the *Drosophila* larval brain, where mutations in key ACD genes caused tumor formation and even metastatic growth (Caussinus and Gonzalez, 2005). *Drosophila* neural stem cells, called neuroblasts (NBs), have become one of the best paradigms in which to analyze the process of ACD (Doe, 2008; Knoblich, 2008). NBs divide asymmetrically to give rise to another NB that retains the self-renewal capacity of the mother stem cell, and a smaller daughter cell called the ganglion mother cell (GMC), which is committed to initiating a process of differentiation. The GMC will divide only once more to generate two neurons or glial cells. A complex protein network regulates this process, ensuring the correct orientation of the mitotic spindle and the basal sorting of cell fate determinants, such as Numb and Prospero (Pros). This regulatory network includes the Par complex, formed by the highly conserved partitioning defective proteins Par6 and Par3 [Bazooka (Baz) in *Drosophila*] and atypical protein kinase C (aPKC), which accumulates at the apical cortex of metaphase NBs (Petronczki and Knoblich, 2001; Schober et al., 1999; Wodarz et al., 2000, 1999). The Par complex associates, through the adaptor protein Inscuteable (Insc), with the Partner of Insc (Pins; LGN or Gpsm2 in mammals) complex, which thereafter orchestrates the proper orientation of the mitotic spindle (Parmentier et al., 2000; Yu et al., 2003). Crucial for this is the activation of the Warts kinase and consequent phosphorylation of the Pins partner Canoe (Cno) (Keder et al., 2015; Speicher et al., 2008). A Rap1-Rgl-Ral small GTPase complex also participates upstream of Cno, anchoring it to the membrane, in regulating asymmetric NB division in the *Drosophila* embryo (Carmena et al., 2011).

In the larval central brain, in the dorsoposterior region of each brain hemisphere, a particular type of NB lineage, called type II NBs (NBIIs), has been described (Bello et al., 2008; Boone and Doe, 2008; Bowman et al., 2008). These NBIIs divide to self-renew and to give rise to an intermediate neural precursor (INP), a transit-amplifying cell, instead of a GMC; the INP, after a period of maturation, divides asymmetrically generating another INP and a GMC. NBII lineages are especially susceptible to overgrowth after a defective asymmetric NB division (Bowman et al., 2008). In addition to ACD regulators having been revealed as tumor suppressors in the larval brain when they are compromised, other *Drosophila* genes originally identified as tumor suppressors have subsequently proven to be key regulators of ACD. This is the case for *lethal (2) giant larvae* [*l(2)gl*], *discs large 1* (*dlg1*), *scribble* (*scrib*) and *brain tumor* (*brat*) (Albertson and Doe, 2003; Bello et al., 2006; Betschinger et al., 2006; Bilder et al., 2000; Bowman et al., 2008; Gateff, 1978, 1994; Lee et al., 2006; Ohshiro et al., 2000; Peng et al., 2000). All this evidence strongly supports a functional link between defects in the process of ACD and tumor formation. Remarkably, all these ACD regulators identified in *Drosophila* have homologs in vertebrates and most of them have been linked with various human cancers (Gómez-López et al., 2014). Moreover, a connection between impairment of ACD and tumorigenesis is also emerging in mouse models and human tumors (Chen et al., 2014; Cicalese et al., 2009; Hwang et al., 2014; Ito et al., 2010; Sugiarto et al., 2011; Wu et al., 2007).

In this study, using the neural stem cells of the *Drosophila* larval brain as a model system, we investigated a potential function of the ACD modulator Cno (afadin, or AF6 in mammals) in tumorigenesis (Miyamoto et al., 1995; Prasad et al., 1993; Speicher et al., 2008). Cno and afadin are cytoplasmic proteins normally associated with adherens junctions in epithelial cells, and they share a conserved modular structure including two Ras-associated (RA) domains (Kuriyama et al., 1996). We show that *cno* loss synergistically interacts with the loss of *scrib* (*Scrib* in mammals), a well-known tumor suppressor gene and ACD regulator (Albertson and Doe, 2003; Bilder et al., 2000). The simultaneous loss of *cno* and *scrib* in NBII clones led to tumor-like overgrowth through both a severe

Instituto de Neurociencias, Consejo Superior de Investigaciones Científicas/Universidad Miguel Hernández, 03550 Sant Joan d'Alacant, Alicante, Spain.
*Present address: Life Sciences Institute, University of Michigan Medical School, Ann Arbor, MI 48109, USA.
‡These authors contributed equally to this work

§Author for correspondence (acarmena@umh.es)

A.C., 0000-0003-1855-7934

Received 15 December 2016; Accepted 1 June 2017

Development (2017) 144, 2570-2583 doi:10.1242/dev.148171

disruption of the ACD process and a *cno* loss-mediated Ras-PI3K-Akt activation. Moreover, in epithelial tissues *cno* also synergistically interacted with *scrib* to promote overgrowth, in this tissue by activating the Ras-Raf-mitogen activated protein kinase (MAPK) pathway. *dlg1* and *l(2)gl*, which are functionally related to *scrib*, did not display such synergism with *cno*. However, they contributed to repress Ras-MAPK signaling in epithelia. The establishment of distinct protein interaction networks among all these tumor suppressor genes, *cno* and the *scrib* module, and the Ras pathway in different developmental contexts is discussed.

RESULTS

cno null mutant NBII clones show disrupted ACD but do not overgrow

We previously found that Cno is expressed in embryonic NBs, where, along with other ACD regulators, it ensures a correct asymmetric NB division. To investigate a potential function of *cno* as a tumor suppressor gene, we first analyzed its expression in larval brain NBs. Cno was detected in both NBI and NBII lineages, and we focused on the latter, which are more prone to manifest tumor-like overgrowth when ACD modulators are compromised (Bowman et al., 2008). Cno was observed along with the transcription factor Deadpan (Dpn), a marker of NBs and INPs, in the cytoplasm of these progenitors at interphase and in a cortical apical crescent at metaphase (Fig. 1A-B′). Cno was also detected at centrosomes throughout mitosis (Fig. 1B-C′).

Given the expression pattern of Cno in NBII lineages, we next investigated the effect of eliminating its function by the mosaic analysis with a repressible cell marker (MARCM) technique (Lee et al., 1999). GFP-labeled wild-type (WT) and cno^{R2} null mutant clones were subjected to a comparative analysis in which different parameters, such as the cellular composition of the clone, the mitotic index of progenitors and the distribution of ACD regulators, were studied. A very characteristic feature of cno^{R2} clones was the reduced size of the NB in 100% of the clones analyzed (Fig. 1D-F). In addition, whereas only one NB, characterized by the simultaneous expression of the transcription factors Dpn and Pointed P1 (PntP1), is always observed in WT clones, extra NBs were occasionally detected in cno^{R2} mutant clones (Fig. 1G-I,N). However, fewer mature INPs and GMCs were present in cno^{R2} clones compared with WT clones (Fig. 1J,K,N). Concomitant with this observation, the mitotic index of progenitor cells was significantly lower in cno^{R2} clones (Fig. 1L). Intriguingly, no significant differences were found in the number of progenitors at interphase (Fig. 1M). These results suggest that, even though in cno^{R2} clones most INPs are entering the cell cycle, not all of them proceed to the mitotic phase or do so at a slower rate than WT INPs.

We next tested the localization of ACD regulators in NBs and INPs of cno^{R2} clones. All of the apical regulators analyzed, the adaptor protein Miranda (Mira), which is required for the basal sorting of the determinants Pros and Brat, but not the cell fate determinant Numb, were mislocalized or absent in metaphase/anaphase NBs of cno^{R2} clones (Fig. 1O-Y). Hence, disruption of asymmetric NB/INP division in cno^{R2} clones might explain the abnormal cellular composition found within these clones.

scrib mutant NBII clones are eliminated by JNK pathway-mediated apoptosis

Despite the ACD defects observed in cno^{R2} clones they did not show tumor growth. Similarly, the loss of other well-known tumor suppressor genes, such as *scrib*, in somatic clones does not lead to any massive overgrowth in epidermal cells; on the contrary, *scrib* mutant clones are eliminated by JNK pathway-mediated apoptosis induced by the surrounding WT tissue (Bilder et al., 2000; Brumby and Richardson, 2003; Igaki et al., 2006). We therefore analyzed the behavior of *scrib* clones in larval brain NBII lineages, a context in which it has not previously been described. $scrib^{1}$ NBII clones were found in only 55% of brains (n=9), as compared with WT clones which appeared in 100% of the brains analyzed (n=10). In addition, $scrib^{1}$ NBII clones were frequently very small (Fig. 2B,B″) compared with WT clones (Fig. 2A,A″). These observations suggested that $scrib^{1}$ NBII clones are dying.

To determine whether, like in *scrib* epithelial clones, the JNK pathway is activated in *scrib* NBII clones and induces their apoptosis we stained them with an antibody to the activated form of JNK (diP-JNK). Compared with WT NBII clones, *scrib* NBII clones showed increased levels of diP-JNK (Fig. 2A-B″). Moreover, inhibiting the JNK pathway in $scrib^{1}$ clones by expressing a dominant-negative form of Basket (Bsk^{DN}), the *Drosophila* JNK homolog, increased the number of $scrib^{1}$ NBII clones, which appeared in 71% of the brains analyzed (n=7); additionally, 44.4% of these clones (n=18 clones of six different brains) were larger than $scrib^{1}$ clones and with lower levels of diP-JNK (Fig. 2D-E″). No effect was observed after overexpressing Bsk^{DN} in otherwise WT clones (Fig. 2C-C″). Hence, all these data indicate that *scrib* NBII clones are eliminated by JNK pathway-mediated apoptosis.

cno scrib double-mutant NBII clones display tumor-like overgrowth

It is generally accepted that cancer is a multistep process, in which multiple genome alterations are required to render a carcinogenic phenotype (Hanahan and Weinberg, 2000, 2011). In *Drosophila*, the first demonstration of cooperative tumorigenesis came from studies in which mutations in tumor suppressor genes, with altered cell polarity, showed neoplastic tumor growth in combination with the constitutive activation of the oncogene *Ras85D* ($Ras85D^{V12}$ or Ras^{V12}) (Brumby and Richardson, 2003; Pagliarini et al., 2003). Given that cooperation between two oncogenes or two tumor suppressor genes can also lead to hyperplasia or neoplasia (Briggs et al., 2008; Land et al., 1983; Liu et al., 2014), we considered whether the simultaneous loss of *scrib* and *cno* in clones could lead to a tumor-like overgrowth. Using the MARCM technique, we generated GFP-labeled cno^{R2} $scrib^{1}$ double-mutant clones in NBII lineages of late third instar larval brains. cno^{R2} $scrib^{1}$ clones showed a striking tumor-like overgrowth, with clone areas significantly larger than those of WT and cno^{R2} or $scrib^{1}$ single-mutant clones (Fig. 3A-E).

Compared with WT clones, the cell population of cno^{R2} $scrib^{1}$ clones appeared very homogeneous. To investigate the composition of these clones, we used antibodies against the transcription factors Dpn and Elav, which mark progenitor cells (NBs and INPs) and differentiated cells (neurons), respectively. WT clones never contained more than 30 (average of 21) progenitor (Dpn^{+}) cells (n=23). Then, taking this number as a reference, we distinguished in cno^{R2} $scrib^{1}$ clones (n=37) two main groups: one (49%, n=18) that did not overgrow (i.e. contained fewer than 30 Dpn^{+} cells); and one (51%, n=19) that did overgrow (i.e. contained more than 30 Dpn^{+} cells). Within this latter group, some mutant clones (27%) showed massive overgrowth (more than 100 Dpn^{+} cells per clone) (Fig. 3F-K). Remarkably, independently of the number of Dpn^{+} cells, all cno^{R2} $scrib^{1}$ clones were composed almost exclusively of progenitor (Dpn^{+}) cells, with very few differentiated ($Elav^{+}$) cells.

Next, we analyzed in more detail whether the progenitor cells present in the double-mutant clones were NBs, INPs or a mix of

Development (2017) 144, 2570-2583 doi:10.1242/dev.148171

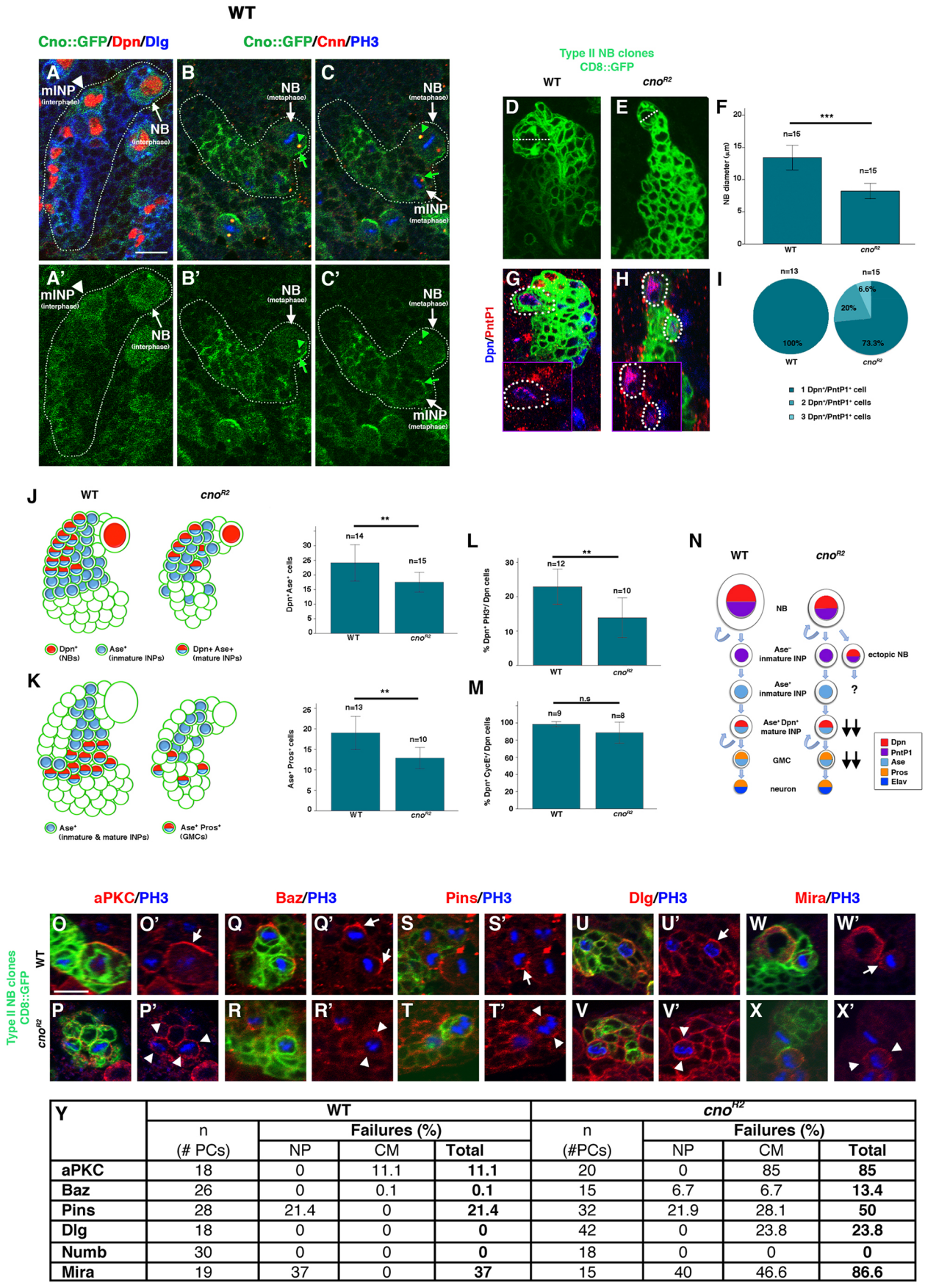

Y	WT				cnoR2			
	n (# PCs)	Failures (%)			n (#PCs)	Failures (%)		
		NP	CM	Total		NP	CM	Total
aPKC	18	0	11.1	**11.1**	20	0	85	**85**
Baz	26	0	0.1	**0.1**	15	6.7	6.7	**13.4**
Pins	28	21.4	0	**21.4**	32	21.9	28.1	**50**
Dlg	18	0	0	**0**	42	0	23.8	**23.8**
Numb	30	0	0	**0**	18	0	0	**0**
Mira	19	37	0	**37**	15	40	46.6	**86.6**

Fig. 1. See next page for legend.

Development (2017) 144, 2570-2583 doi:10.1242/dev.148171

Fig. 1. *cno* null NBII clones do not overgrow. (A,A′) GFP-labeled endogenous Cno is at low levels in interphase NBs (arrow) and INPs (arrowhead) of NBII lineages (dotted line); Dpn marks progenitors (NBs and INPs). (B-C′) At metaphase, Cno is enriched in cortical crescents in progenitors (green arrows); Cno is also detected in centrosomes (green arrowheads), as labeled by Centrosomin (Cnn); phospho-Histone H3 (PH3) marks mitotic cell DNA. B and C show the same clone at different confocal planes of focus. (D-F) NBs (dotted line indicates NB diameter) in cno^{R2} versus WT clones (D,E) are significantly smaller (F; *n*, number of clones from 5 WT or 8 cno^{R2} brains analyzed). (G-I) In WT clones, only one Dpn^+ $PntP1^+$ NB (dotted line) is present; the inset shows the NB expressing both factors (G); in cno^{R2} clones two or three NBs are occasionally detected (H,I; *n*, number of clones of 9 WT and 11 cno^{R2} brains). (J,K) Numbers of mature INPs (Dpn^+ Ase^+) (J) and GMCs (Ase^+ $Pros^+$) (K) are significantly lower in cno^{R2} clones (*n*, number of clones from 5 or 6 WT and from 8 or 6 cno^{R2} brains in J or K). (L,M) The progenitor cell mitotic index is significantly lower in cno^{R2} clones (L), whereas there are no significant differences in the number of interphase progenitors (M); *n*, number of clones of 6 or 5 WT and 6 or 5 cno^{R2} brains in L or M. Data in F,J-M were analyzed by Student's *t*-test. ***P<0.001, **P<0.01; n.s, not significant. Error bars indicate s.d. (N) Comparison of WT and cno^{R2} clones. (O-Y) Defects and quantification of ACD regulator (red) localization (arrowheads) in cno^{R2} clones; in WT clones, regulators are enriched in cortical crescents (arrows) of metaphase/anaphase progenitors. PCs, progenitor cells; NP, not present; CM, cortical mislocalization. Scale bars: 10 µm.

both. We observed that, whereas in WT clones there was always only 1 NB (Dpn^+ $PntP1^+$) and an average of 4.7 immature INPs (iINPs; Dpn^- $PntP1^+$) (*n*=13), cno^{R2} $scrib^1$ clones showed significantly more NBs and iINPs, with a mean value of 7.5 NBs and 7.7 iINPs (*n*=18); this value increased to 12.4 NBs and 10.1 iINPs when considering the overgrowing population of double-mutant clones (*n*=7), and even in the non-overgrowing population the mean value was 4.3 NBs and 6 iINPs (*n*=11) (Fig. 3L-Q). To further characterize cno^{R2} $scrib^1$ clones, we tested the number of mature INPs (mINPs). Whereas in WT clones (*n*=14) mINPs (Dpn^+ Ase^+) represented 53% of the whole Ase^+ cell population, in cno^{R2} $scrib^1$ clones (*n*=12) mINPs represented 44%, decreasing to 38% in the double-mutant clone population that showed massive overgrowth (*n*=8) (Fig. 3R-V). Given the greater number of NBs and iINPs in cno^{R2} $scrib^1$ clones compared with WT clones, this result (the decrease in the number of mINPs in double-mutant clones) might suggest that INPs do not mature properly and tend to revert to a more undifferentiated state. The numbers of each of these cell types (NBs, iINPs and mINPs) in cno^{R2} or $scrib^1$ single-mutant clones were significantly different from those in the overgrowing population of cno^{R2} $scrib^1$ clones (Fig. 3K,P,Q,V).

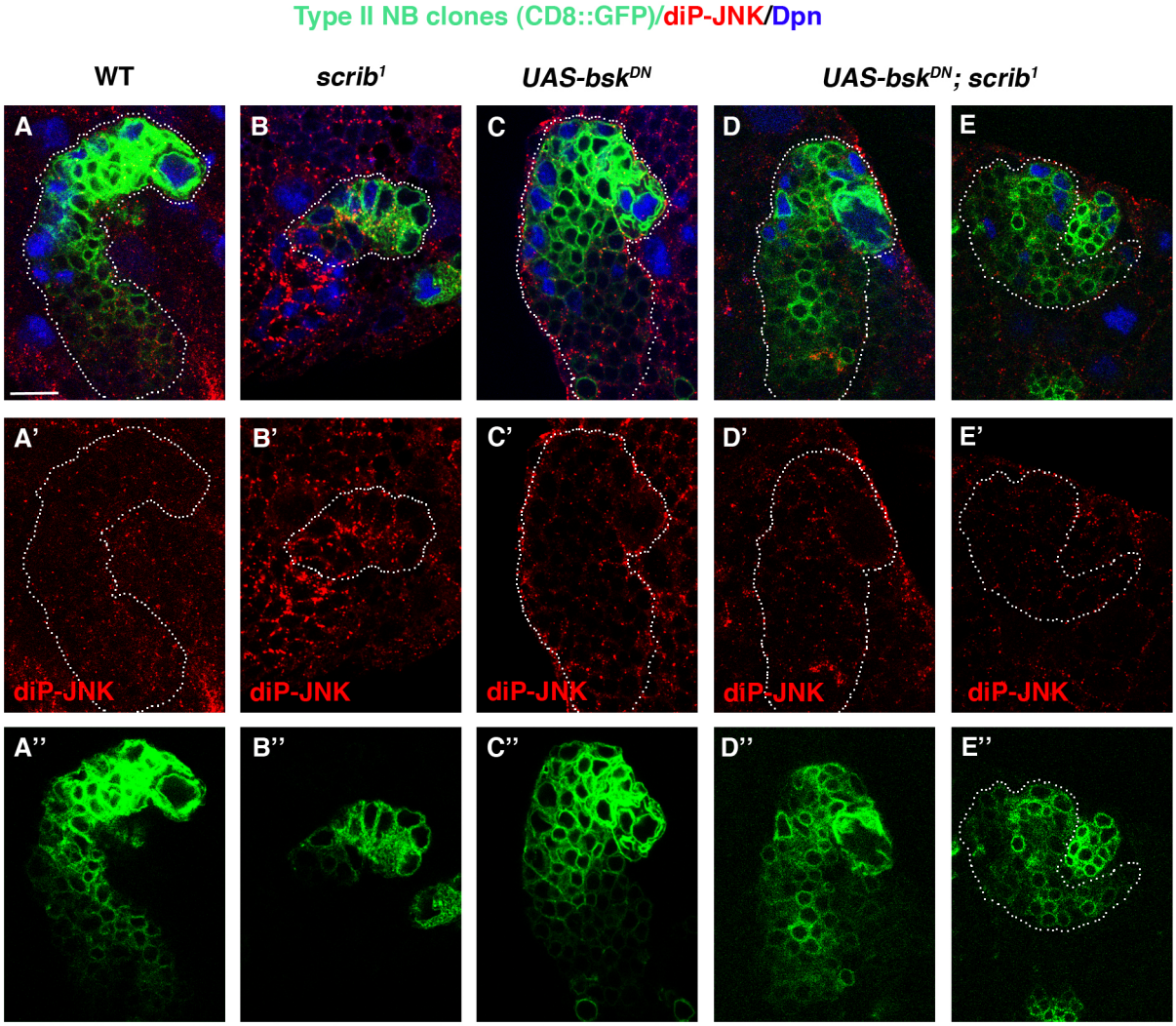

Fig. 2. *scrib* NBII clones are eliminated by JNK-mediated apoptosis. (A-E) GFP-labeled NBII clones (green, single channel in A″-E″) of WT (A), $scrib^1$ (B), bsk^{DN} (C) and bsk^{DN} in a $scrib^1$ mutant background (D,E) stained for Dpn and diP-JNK (red, single channel in A′-E′). (A-B″) $scrib^1$ clones are smaller than WT clones and upregulate diP-JNK. (C-C″) bsk^{DN} expression in a WT background has no apparent phenotype. (D-E″) bsk^{DN} expression partially rescues the $scrib^1$ phenotype (two different examples are shown). Scale bar: 10 µm.

Development (2017) 144, 2570-2583 doi:10.1242/dev.148171

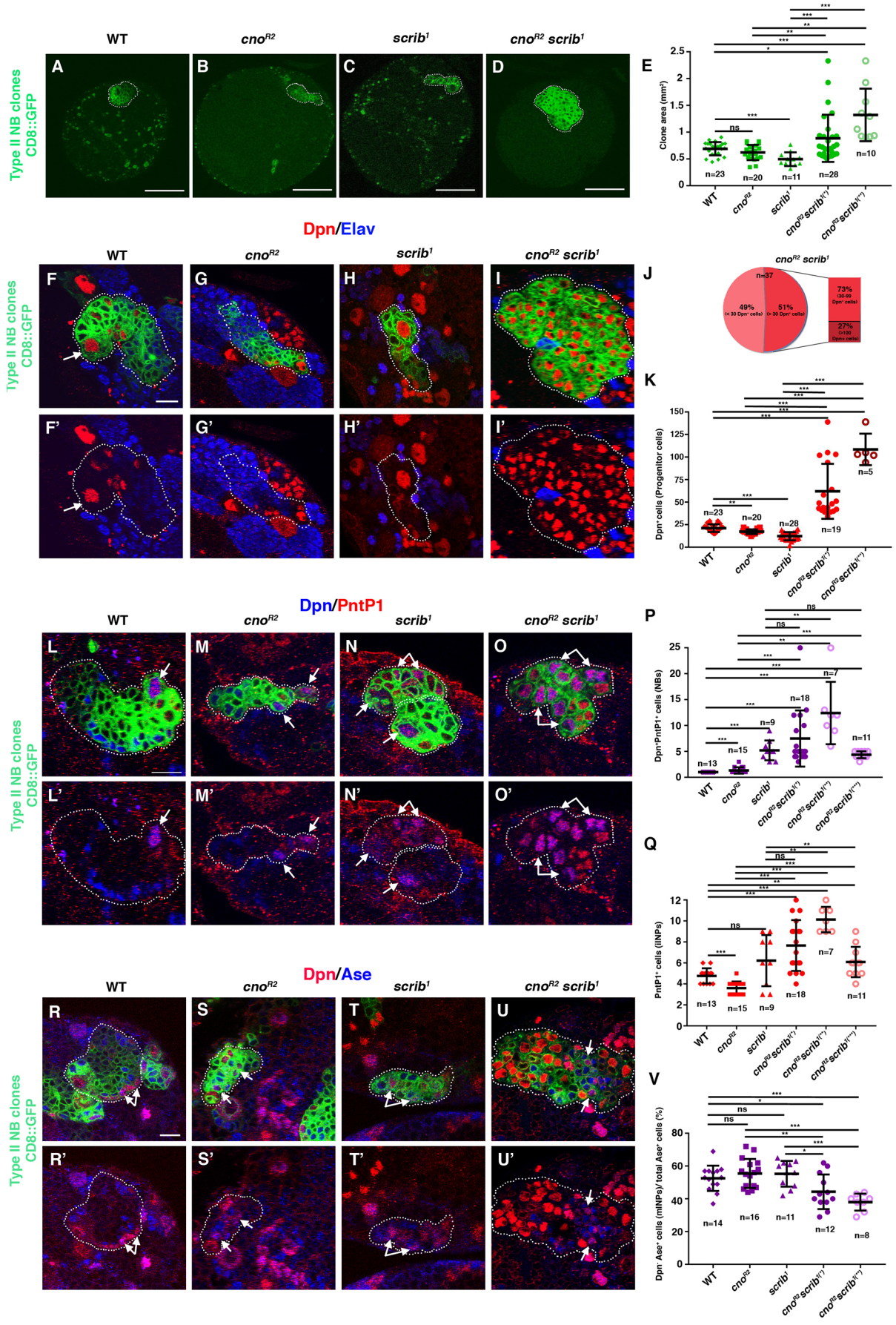

Fig. 3. See next page for legend.

Development (2017) 144, 2570-2583 doi:10.1242/dev.148171

Fig. 3. *cno scrib* NBII clones display tumor-like overgrowth. (A-E) Brain hemispheres showing a WT (A), cno^{R2} (B), $scrib^{1}$ (C) or cno^{R2} $scrib^{1}$ (D) clone, and quantification of the clone area (E; *n*, number of clones analyzed, each clone from different brains). (F-I′) WT NBII clones show a large Dpn^{+} cell, which is the NB (arrow), some smaller Dpn^{+} INPs and several $Elav^{+}$ neurons within the clone (F,F′). cno^{R2} and $scrib^{1}$ clones show fewer progenitor cells (G-H′). cno^{R2} $scrib^{1}$ clones contain mainly Dpn^{+} progenitors and very few $Elav^{+}$ neurons (I,I′). (J,K) Quantification of Dpn^{+} cells (*n*, number of clones of 19, 13, 9, 9 and 9 brains of the indicated genotypes). (L-Q) WT NBII clones show just one Dpn^{+} $PntP1^{+}$ NB (arrow) and some $PntP1^{+}$ immature INPs (L,L′). cno^{R2} and $scrib^{1}$ single clones show extra NBs (M-N′). cno^{R2} $scrib^{1}$ clone (confocal plane of the whole clone) contains multiple Dpn^{+} $PntP1^{+}$ NBs (arrows in O,O′) and several $PntP1^{+}$ immature INPs, as quantified in P,Q (*n*, number of clones of 10, 10, 8, 16, 7 and 9 brains of the indicated genotypes). (R-U′) Dpn^{+} Ase^{+} mature INPs in WT, cno^{R2} and $scrib^{1}$ NBII clones (arrows in R-T′). In cno^{R2} $scrib^{1}$ clones, fewer mature INPs are detected within the whole Ase^{+} cell population (U,U′), as quantified in V (*n*, number of clones of 9, 9, 11, 10 and 11 brains analyzed). cno^{R2} $scrib^{1}$(*), whole clone population; cno^{R2} $scrib^{1}$ (**), clones with massive overgrowth; cno^{R2} $scrib^{1}$(***), clones with fewer than 30 Dpn^{+} cells per clone. Note that cno^{R2} $scrib^{1}$ (**) clones show significant differences to cno^{R2} and $scrib^{1}$ single-mutant clones in all the analyses. Data (E,K,P,Q,V) were analyzed by Student's *t*-test. ***P<0.001, **P<0.01, *P<0.05; ns, not significant. Error bars indicate s.d. Scale bars: 10 µm, except 50 µm in A-D.

Thus, in summary, the loss of *cno* and of *scrib* synergistically interact in NBII lineages, leading to the formation of a tumor mass that is mainly composed of progenitor cells, with very few differentiated cells.

ACD is substantially altered in *cno scrib* double-mutant NBII clones

Like Cno, the tumor suppressor Scrib participates in regulating ACD (Albertson and Doe, 2003). Hence, we considered how the simultaneous loss of both modulators in *cno scrib* clones could be affecting this process. We analyzed the localization of the apical protein aPKC and the basal cell fate determinant Numb in progenitors of these mutant clones. The localization of aPKC and Numb failed in 85% and 0% in cno^{R2} clones and in 42.8% and 40% in $scrib^{1}$ clones, respectively (Fig. 4A-B′,D-E′,G; see also Fig. 1O-P′,Y). In cno^{R2} $scrib^{1}$ double-mutant clones, the asymmetric cortical distribution of both ACD regulators at metaphase/anaphase failed in 100% of the progenitors analyzed, with both regulators distributed throughout the cell cortex in most cells of mutant clones (Fig. 4C,C′,F-G). These defects suggest that ACD is severely affected in cno^{R2} $scrib^{1}$ clones and that this could account for the substantial increase in progenitor cells observed in these clones.

cno loss in *cno scrib* mutant NBII clones promotes Ras activation

Despite the strong ACD defects observed in cno^{R2} $scrib^{1}$ clones, it was still unclear how the JNK-mediated apoptosis observed in *scrib* clones was overcome by the absence of Cno. In epithelial tissues, constitutive activation of the oncogene *Ras* (Ras^{V12}) in *scrib* clones entails a change in the JNK pathway outcome from a proapoptotic to a progrowth effect. As a consequence, Ras^{V12} *scrib* clones massively overgrow (Brumby and Richardson, 2003; Igaki et al., 2006). Intriguingly, Cno binds directly to Ras through its RA domains (Kuriyama et al., 1996), and we have previously shown that Cno represses the Ras signaling pathway during muscle and heart progenitor specification (Carmena et al., 2006). Hence, we considered whether Ras would be upregulated in *cno scrib* NBII clones, contributing in combination with *scrib* loss to the tumor-like overgrowth observed.

To test this hypothesis, we expressed a dominant-negative form of Ras (Ras^{DN}) in cno^{R2} $scrib^{1}$ clones. In this genetic background, the total number of progenitor (Dpn^{+}) cells significantly decreased to 24.4 (*n*=14 clones), as compared with the 48.6 progenitor cells observed in cno^{R2} $scrib^{1}$ clones (*n*=20) (Fig. 4H-L). We also performed this experiment expressing Ras^{RNAi} to knock down Ras in the cno^{R2} $scrib^{1}$ mutant background with a similar result (Fig. 4M-Q). The loss of Ras in an otherwise WT NBII clone did not have any consequences for clone morphology, size or the number of progenitor cells (Fig. 4I,N,S,L,Q,V). Reducing Ras levels in cno^{R2} clones did not significantly affect the number of progenitors, but the morphology and size of the clones/NBs were overall more similar to those of WT clones (Fig. 4T-V).

To further support an effect of *cno* loss on Ras upregulation in cno^{R2} $scrib^{1}$ clones, we expressed in this mutant background either a WT form of Cno (Cno^{WT}) or a form that lacks the two RA domains ($Cno^{\Delta N}$). Whereas the expression of Cno^{WT} rescued the cno^{R2} $scrib^{1}$ overgrowth phenotype (mean of 17.7 Dpn^{+} cells per clone, as compared with 51.8 in cno^{R2} $scrib^{1}$ clones), no significant effect was observed after expressing $Cno^{\Delta N}$ (Fig. 4W-Z).

All these data strongly support that (1) *cno* loss in cno^{R2} $scrib^{1}$ clones leads to Ras activation, which suppresses *scrib* loss-induced cell death, and (2) that the severe defects in ACD observed in cno^{R2} $scrib^{1}$ clones without Ras activation are insufficient to cause tumor-like overgrowth in cno^{R2} $scrib^{1}$ clones.

Ras^{V12} *scrib* mutant NBII clones survive but do not overgrow

As mentioned above, Ras^{V12} *scrib* clones promote overgrowth in epithelial tissues (Brumby and Richardson, 2003; Pagliarini et al., 2003). Given that in NBII lineages cno^{R2} loss induced Ras activation and tumor-like overgrowth in a $scrib^{1}$ background, we tested the effect of directly expressing Ras^{V12} on *scrib* NBII clones in larval brains. Whereas *scrib* clones were eliminated by apoptosis and were rarely detected (see above), Ras^{V12} *scrib* mutant clones survived, appearing at a similar rate to WT clones. Whereas in WT clones there was always only 1 NB (Dpn^{+} Ase^{-}) per clone (*n*=12), in Ras^{V12} *scrib* clones 2 or 3 NBs were found in 18.2% or 36.3%, respectively, of the clones analyzed (*n*=11) (Fig. 4AA-DD). Despite these defects in the number of NBs, and contrary to what occurs in epithelial tissues, Ras^{V12} *scrib* NBII clones did not show overgrowth.

Altogether, from these and the previous results we conclude that the tumor-like overgrowth of cno^{R2} $scrib^{1}$ NBII clones does not rely only on *cno* loss-mediated Ras derepression or on the severe ACD defects observed, but on both of them (see Discussion).

cno loss in *cno scrib* mutant NBII clones activates the Ras-PI3K-Akt pathway

In epithelia, Ras^{V12} signals through the Raf-MAPK pathway to promote overgrowth (Brumby and Richardson, 2003). Thus, to confirm the effect of *cno* loss on Ras activation, we assessed the levels of diP-MAPK (a Ras-Raf-MAPK pathway activity readout) in cno^{R2} $scrib^{1}$ NBII clones. No diP-MAPK was detected in these or control clones, and it was at low levels or undetectable in Ras^{V12} NBII clones (Fig. S1). These results indicate that the Ras-Raf-MAPK pathway is not normally active in WT NB clones and that the ectopic activation of Ras in cno^{R2} $scrib^{1}$ NBII clones is barely able to induce this pathway. In fact, the expression of Raf^{RNAi} in a cno^{R2} $scrib^{1}$ mutant background had no significant effect on reducing the cno^{R2} $scrib^{1}$ overgrowth phenotype, as apparent from analyzing the number of progenitor (Dpn^{+}) cells (*P*=0.12) (Fig. 5A-C).

Development (2017) 144, 2570-2583 doi:10.1242/dev.148171

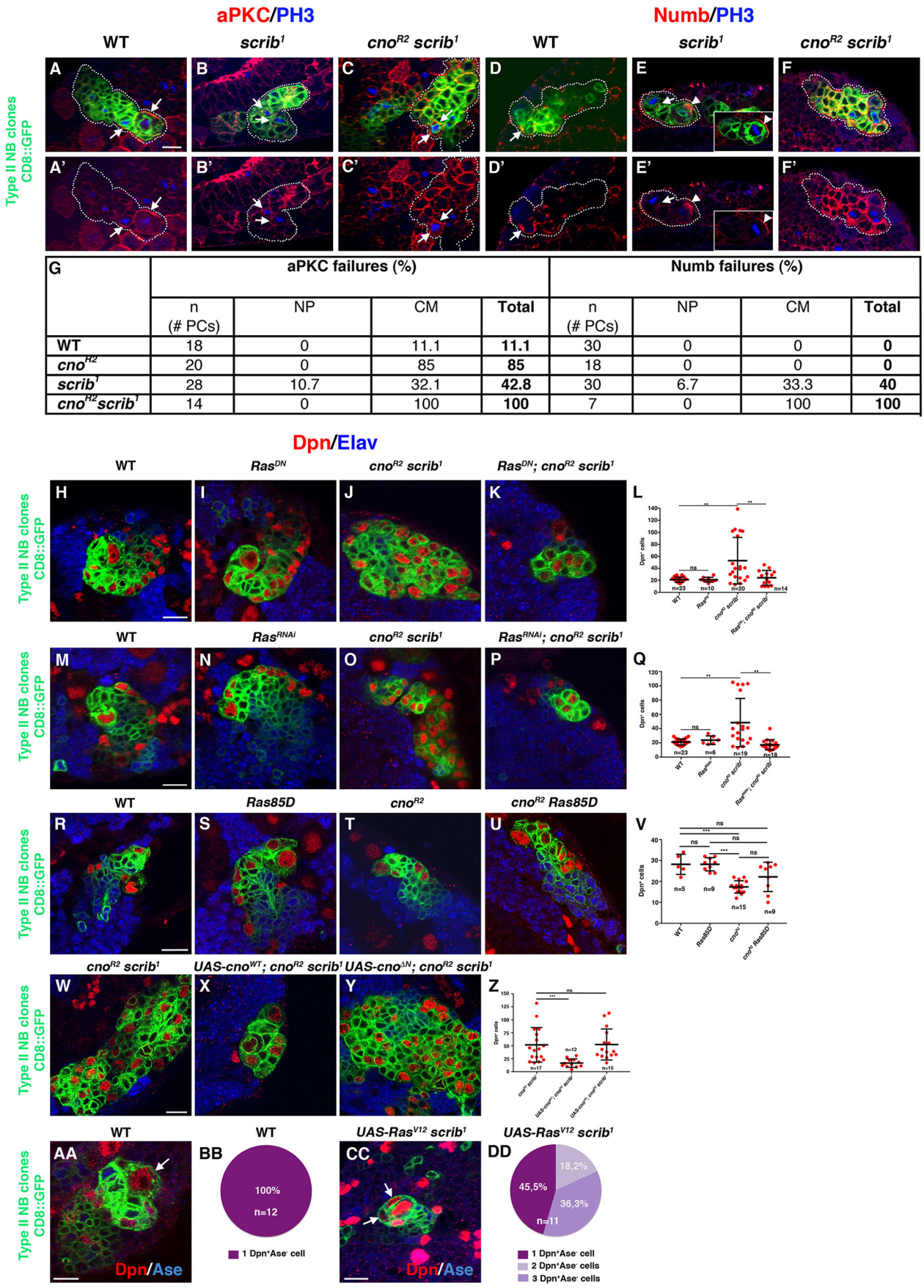

G	aPKC failures (%)				Numb failures (%)			
	n (# PCs)	NP	CM	**Total**	n (# PCs)	NP	CM	**Total**
WT	18	0	11.1	**11.1**	30	0	0	**0**
cno^{R2}	20	0	85	**85**	18	0	0	**0**
scrib^{1}	28	10.7	32.1	**42.8**	30	6.7	33.3	**40**
cno^{R2}scrib^{1}	14	0	100	**100**	7	0	100	**100**

Fig. 4. See next page for legend.

Development (2017) 144, 2570-2583 doi:10.1242/dev.148171

Fig. 4. *cno scrib* NBII clones show severe defects in ACD and the upregulation of Ras activity. (A-F′) WT, *scrib*^{1} and *cno*^{R2} *scrib*^{1} NBII clones stained for aPKC and PH3 (A-C′) or Numb and PH3 (D-F′). In WT clones, aPKC and Numb are asymmetrically enriched in dividing progenitors (arrows in A,A′,D,D′). *scrib*^{1} clones show defects in the localization of both aPKC and Numb (arrows in B,B′,E,E′); arrowhead points to a Numb crescent correctly formed in the NB, which is better seen in the inset (another focal plane of the same clone). In *cno*^{R2} *scrib*^{1} NBII clones, both aPKC and Numb are always in extended crescents at the cortex of clone cells (arrows in C,C′,F,F′). (G) Quantification of aPKC and Numb localization defects in the specified genotypes. PCs, progenitor cells; NP, not present; CM, cortical mislocalization. (H-Z) Dpn labels progenitor cells and Elav labels differentiated cells (neurons). The tumor-like overgrowth shown by *cno*^{R2} *scrib*^{1} NBII clones (J,O,W) is significantly suppressed by reducing Ras activity (K,L,P,Q) and by expressing a *cno* WT form (X,Z), but it is not altered by expressing a *cno* form lacking the Ras-associated (RA) domains (*cno*$^{\Delta N}$) (Y,Z). Eliminating or reducing Ras activity in WT or *cno*^{R2} clones does not have any significant effect on progenitor cell number (H,I,L-N,Q-V). *n*, number of clones of 18, 8, 14 and 9 (L), 19, 6, 15 and 14 (Q), 4, 8, 8 and 5 (V) or 16, 9 and 11 (Z) brains. Data in L,Q,V,Z were analyzed by Student's *t*-test. ***P<0.001, **P<0.01; ns, not significant. Error bars indicate s.d. (AA-DD) WT NBII clones always contain one NB (AA arrow, BB). In *UAS-Ras*^{V12} *scrib*^{2} NBII clones extra NBs are detected (CC arrows, DD). *n*, number of clones analyzed of 8 WT and 8 mutant clone brains. Scale bars: 10 µm.

Apart from the Raf-MAPK pathway, other effectors of Ras have been described, such as the phosphatidylinositol-3 kinase (PI3K)-Akt pathway (Fig. 5D). Hence, we examined whether this pathway was exerting the effects of ectopic Ras activation in *cno*^{R2} *scrib*^{1} NBII clones. The expression of *Akt*^{RNAi} in that mutant background dramatically rescued the overgrowth phenotype of *cno*^{R2} *scrib*^{1} clones, with an average of 20 Dpn^{+} cells per clone as compared with 51.8 in the double mutant (Fig. 5E-G). The loss of Akt in an otherwise WT NBII clone did not have any effect on clone size, morphology or progenitor cell number (Fig. S2). We also directly measured Akt signaling activation in *cno*^{R2} *scrib*^{1} clones by analyzing phospho-Akt (pAkt) levels. Western blotting of WT brains versus those with *cno*^{R2} *scrib*^{1} clones showed higher levels of the pAkt 66 kDa isoform in the latter (Fig. 5H). Hence, the ectopic Ras induced by *cno* loss in *cno*^{R2} *scrib*^{1} NBII clones leads to PI3K-Akt pathway activation (see Discussion).

cno scrib mutant clones in epithelia overgrow and activate the Ras-Raf-MAPK pathway

To determine a potential context-dependent effect of *cno* loss on Ras activation and tumor induction in a *scrib* mutant background, we analyzed *cno scrib* clones in epithelial tissues, which grow by symmetric cell divisions. *cno*^{R2} *scrib*^{1} clones induced in antennal discs showed a clear tumor overgrowth in 28% of the clones analyzed (n=14), whereas no overgrowth was observed in WT (n=12) or *cno*^{R2} (n=10) clones, and *scrib*^{1} clones overgrew in 6.7% of cases (n=15). *Ras*^{V12} *scrib* clones showed tumor overgrowth in 100% of the clones analyzed (n=20) (Fig. 6A-L). Hence, the *cno*^{R2} *scrib*^{1} phenotype was similar, although with less penetrance and expressivity, to that described for *Ras*^{V12} *scrib* in epithelial tissues.

As mentioned above, in epithelia Ras^{V12} signals through the Raf-MAPK pathway to promote overgrowth (Brumby and Richardson, 2003). Thus, we tested whether *cno* loss induces the Ras-MAPK pathway in this epithelial context. By immunofluorescence, neither *cno*^{R2} nor *scrib*^{1} single-mutant clones showed any apparent diP-MAPK upregulation compared with WT clones (Fig. 6A′-C′). However, both *cno*^{R2} *scrib*^{1} and *Ras*^{V12} *scrib* antennal clones exhibited diP-MAPK upregulation, the former to a lesser extent than the latter (Fig. 6D′,F′). Hence, in epithelial tissues the *cno*^{R2} *scrib*^{1} and *Ras*^{V12} *scrib* mutant clone overgrowth phenotypes are more similar than in NBs (see Discussion). Intriguingly, quantification of diP-MAPK levels in *cno*^{R2} or *scrib*^{1} single-mutant disc extracts showed, on average, about a fivefold or sevenfold increase, respectively, in MAPK activation relative to WT discs (Fig. 6M,N). This result strongly supports a repressive effect of both Cno and Scrib on Ras-MAPK signaling pathway in epithelia (see also Dow et al., 2008).

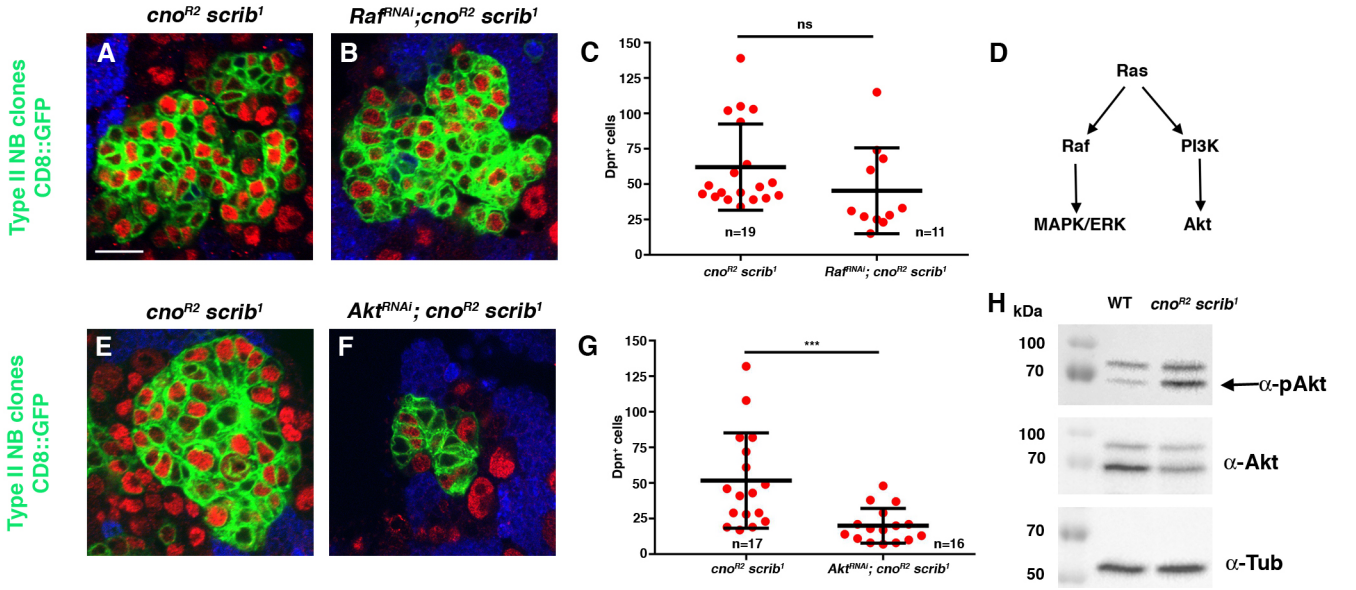

Fig. 5. *cno* loss in *cno scrib* NBII clones activates the Ras-PI3K-Akt pathway. (A-G) The tumor-like overgrowth shown by *cno*^{R2} *scrib*^{1} NBII clones is not altered by reducing the Ras effector Raf (A-C; *n*, number of clones of 15 and 10 brains analyzed), but it is significantly suppressed by downregulating the Ras effector Akt (E-G; *n*, number of clones of 10 and 9 brains). Data in C,G were analyzed by Student's *t*-test. ***P<0.001; ns, not significant. Error bars indicate s.d. (D) In *Drosophila*, Ras normally triggers the Raf-MAPK pathway but can also activate the PI3K-Akt signaling pathway in particular conditions (Prober and Edgar, 2002). (H) Western blot of larval brain lysates with NBII clones of the indicated genotype showing pAkt levels. Two isoforms of Akt are detected by the antibody (66 and 85 kDa); the 66 kDa isoform is activated in *cno*^{R2} *scrib*^{1} clones (arrow). Scale bar: 10 µm.

Development (2017) 144, 2570-2583 doi:10.1242/dev.148171

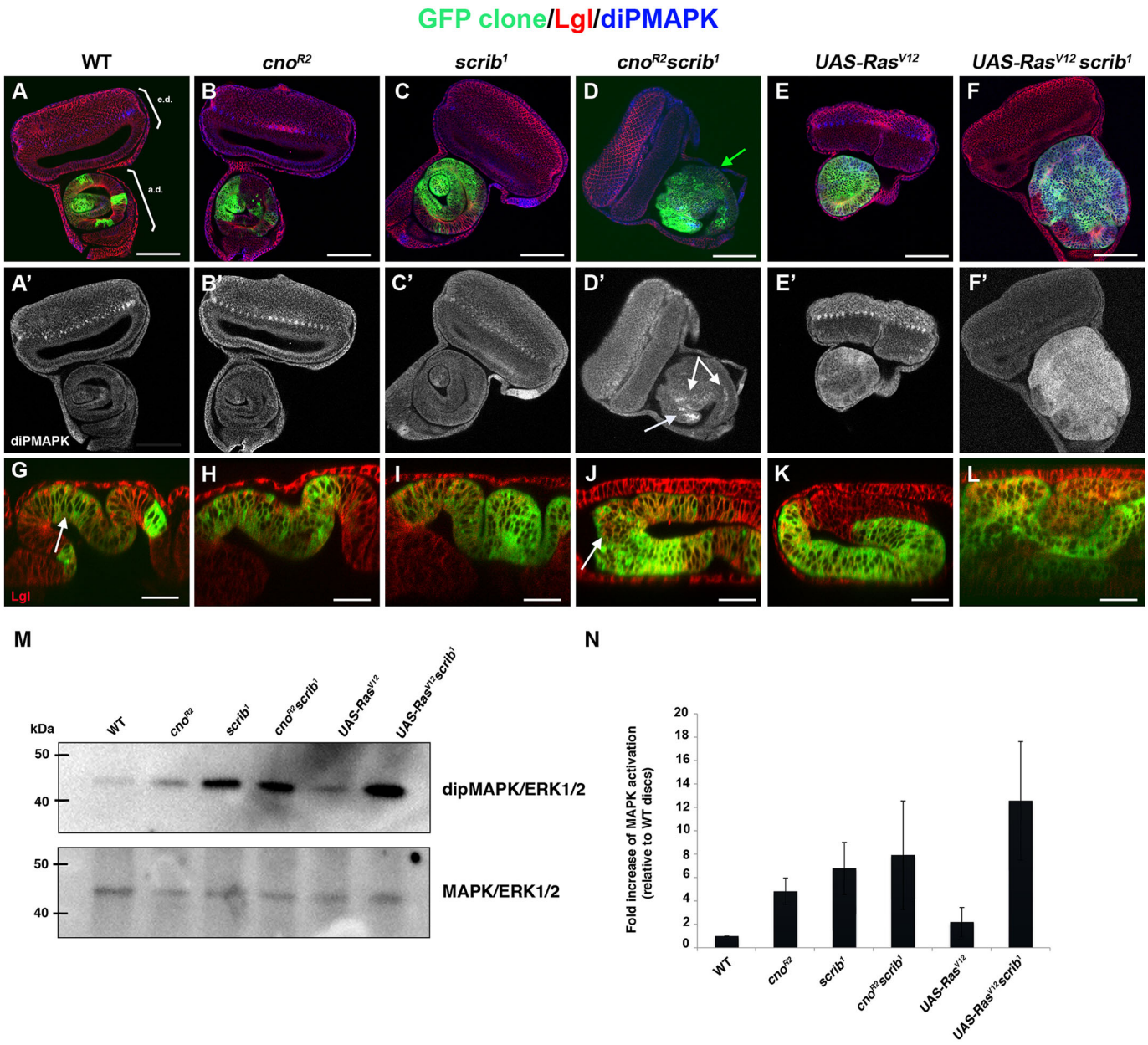

Fig. 6. *cno scrib* clones in epithelial tissues overgrow and activate the Ras-MAPK pathway. (A-F′) Confocal sections of eye-antennal discs showing GFP-labeled antennal disc clones of the specified genotypes stained for L(2)gl and diP-MAPK (A-F). e.d., eye disc; a.d., antennal disc. Whereas WT (A), cno^{R2} (B) or $scrib^{1}$ (C) clones do not overgrow, cno^{R2} $scrib^{1}$ clones in antennal discs show overgrowth (arrow in D); Ras^{V12} (E) and Ras^{V12} $scrib^{1}$ (F) clones also show overgrowth, the latter to a greater extent than cno^{R2} $scrib^{1}$ clones. diP-MAPK is not detected in WT (A′), cno^{R2} (B′) or $scrib^{1}$ (C′) antennal disc clones but it is present in cno^{R2} $scrib^{1}$ clones (arrows in D′), in Ras^{V12} (E′) and to a higher extent in Ras^{V12} $scrib^{1}$ (F′). (G-L) Antennal disc sagittal views showing the altered rounded cell morphology in mutant clones (arrow in J), compared with the columnar cell morphology in WT clones (arrow in G). (M) Western blot of eye-antennal imaginal disc lysates of the indicated genotypes showing diP-MAPK and MAPK levels. (N) Fold increase of MAPK activation in the indicated genotypes relative to WT. Error bars indicate s.d. (n=3 independent experiments). Scale bars: 50 µm (A-F′); 10 µm (G-L).

Dlg1 and L(2)gl repress Ras-MAPK signaling in epithelia without synergistically interacting with Cno

Scrib functions along with the tumor suppressors Dlg1 and L(2)gl in a common pathway to regulate cell polarity and growth in epithelial tissues (Bilder et al., 2000; Elsum et al., 2012). Moreover, not only *scrib* but also *dlg1* and *l(2)gl* cooperate with Ras^{V12} to promote neoplastic overgrowth (Brumby and Richardson, 2003; Pagliarini et al., 2003). Thus, we considered whether *cno* loss would also synergistically interact with *dlg1* and *l(2)gl* mutants in imaginal discs to induce tumor formation. $dlg1^{RNAi}$; cno^{R2} and $l(2)gl^{RNAi}$; cno^{R2} double-mutant clones in antennal discs showed consistent overgrowth and upregulation of diP-MAPK in 100% of the clones analyzed (Fig. 7A,A′,E-F′). The localization of Scrib was also disturbed (Fig. 7G′,K′-L′). Intriguingly, $dlg1^{RNAi}$ and $l(2)gl^{RNAi}$ single-mutant clones already displayed this phenotype (Fig. 7C-D′,I-J′). Hence, the loss of *cno* in both $dlg1^{RNAi}$ and $l(2)gl^{RNAi}$ genetic backgrounds seemed to slightly exacerbate the phenotype of each single-mutant condition, especially in terms of altered cellular morphology and tissue disorganization (Fig. 7G-L), although the effect did not seem to be

Development (2017) 144, 2570-2583 doi:10.1242/dev.148171

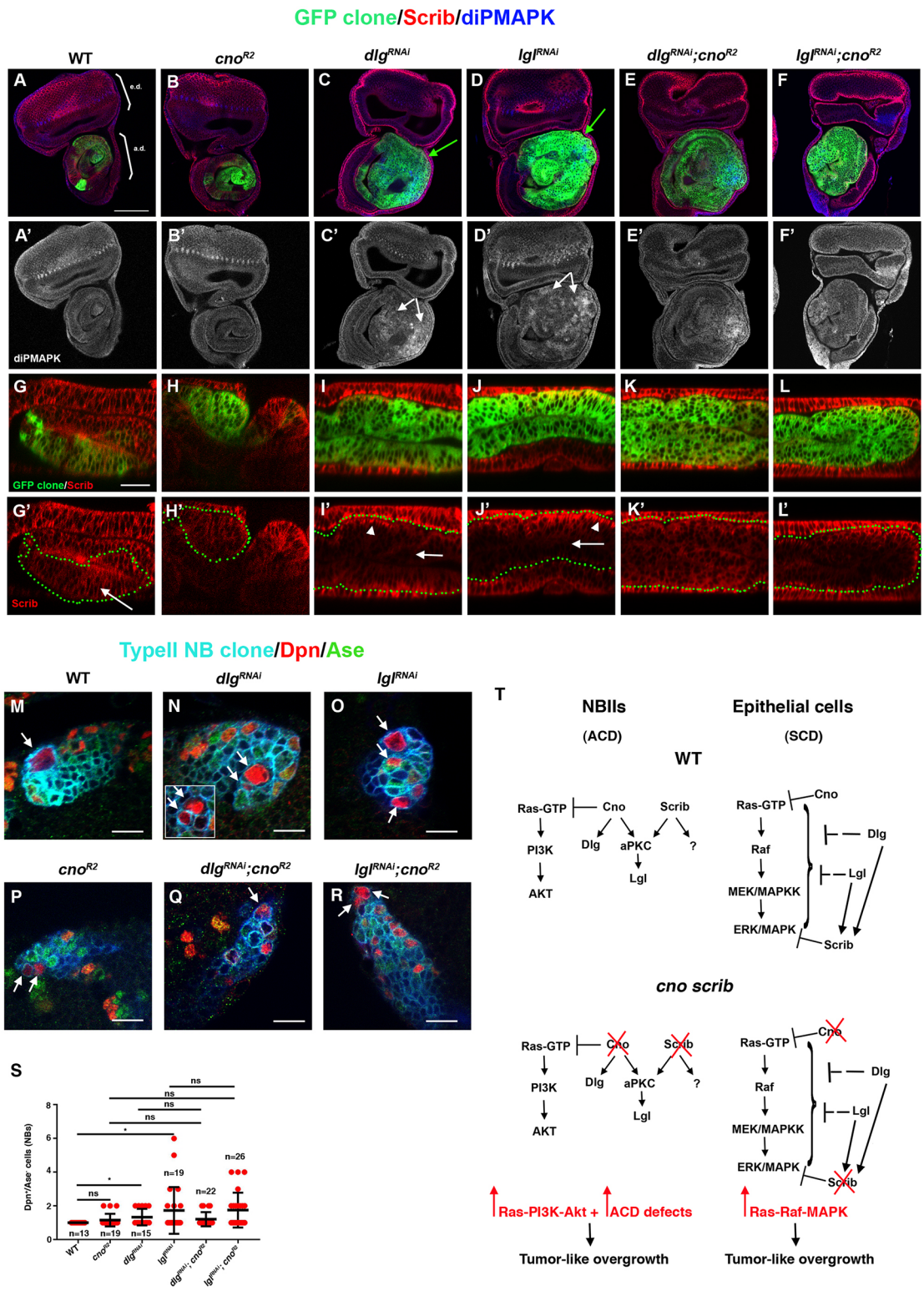

Fig. 7. See next page for legend.

synergistic, as it was clearly observed in *cno*^{R2} *scrib*^{1} antennal disc clones (see Discussion).

Finally, we wanted to determine the behavior of *dlg1*^{RNAi}*; cno*^{R2} and *l(2)gl*^{RNAi}*; cno*^{R2} double-mutant NBII clones. Both *dlg1*^{RNAi} and *l(2)gl*^{RNAi} single-mutant NBII clones had extra NBs compared with control NBII clones, but they did not overgrow (Fig. 7M-O,S). In fact, in the case of *l(2)gl*^{RNAi} clones, and despite the extra NBs (up to 7), the clones appeared smaller than control clones. Intriguingly, both *dlg1*^{RNAi}*; cno*^{R2} and *l(2)gl*^{RNAi}*; cno*^{R2} double-mutant NBII clones displayed a phenotype that was more similar to that of *cno*^{R2} single-mutant clones (i.e. 100% of the clones showed an undersized NB, which is a very characteristic feature of *cno*^{R2} NBII clones) with

Development (2017) 144, 2570-2583 doi:10.1242/dev.148171

Fig. 7. Dlg1 and L(2)gl repress Ras-MAPK signaling in epithelia. (A-F′) Confocal sections of eye-antennal discs showing GFP-labeled clones of the indicated genotypes stained for Scrib and diP-MAPK (A-F). e.d., eye disc; a.d., antennal disc. *dlg1* and *l(2)gl* clones show overgrowth (arrows in C, D) and an upregulation of diP-MAPK (arrows in C′,D′), a phenotype that it is not exacerbated in *dlg1*, cno^{R2} or *l(2)gl* cno^{R2} double-mutant clones (E-F′). (G-L) Antennal disc sagittal views showing the altered rounded cell morphology in mutant clones. (G′-L′) Defects in Scrib expression and localization are found in *dlg1* and *l(2)gl* clones (arrows and arrowheads in I′,J′) compared with WT clones (G′). Green dotted lines delineate the clones. (M-R) In WT NBII clones, only one large NB (Dpn^+ Ase^-) is detected (arrow in M). In *dlg1* clones, extra NBs are occasionally detected (arrows in N; the inset shows a deeper confocal plane of focus). In *l(2)gl* clones, several extra NBs are present (arrows in O) and clones are smaller than WT clones. (P-R) $dlg1^{RNAi}$ cno^{R2} (Q) and $l(2)gl^{RNAi}$ cno^{R2} (R) clones present a small NB and sometimes extra NBs (arrows), like *cno* single-mutant clones (P), as quantified in S (*n*, number of clones of 13, 19, 15, 22 and 26 brains analyzed of the indicated genotypes). Data were analyzed by Student's *t*-test. **P*<0.05; ns, not significant. Error bars indicate s.d. Scale bars: 50 µm (A-F′); 10 µm (G-R). (T) Diagrams depicting distinct protein interaction networks among Cno, the Scrib module [Scrib, Dlg1 and L(2)gl] and the Ras pathway in different developmental contexts (NBIIs versus epithelial cells) and in distinct genetic backgrounds (WT versus *cno scrib* double mutants). Arrows indicate epistatic relationships. In WT NBIIs, Cno directly represses Ras by physically interacting with Ras-GTP. While Cno is epistatic to Dlg1 and L(2)gl, Cno and Scrib act in parallel or partially convergent pathways. In WT epithelial cells, Cno, Scrib, Dlg1 and L(2)gl cooperate to repress the Ras-MAPK pathway: Cno and Scrib repress it by directly binding Ras-GTP and MAPK, respectively; Dlg1 and L(2)gl repress it indirectly by contributing to Scrib localization and by other (direct or indirect) unknown mechanism(s) (dashed line). In *cno scrib* double-mutant NBIIs, both the upregulation of the Ras-PI3K-Akt pathway and the strong defects in ACD lead to a tumor-like overgrowth; in *cno scrib* mutant epithelia, the upregulation of the Ras-Raf-MAPK pathway promotes the tumor-like overgrowth.

no apparent overgrowth (Fig. 7P-R). We tested the levels of Dlg1 and L(2)gl proteins in NBII clones after overexpressing their RNAi, and observed strong reduction or elimination (Fig. S3). Hence, as in epithelia, in NBII lineages *cno* did not synergistically interact with *dlg1* or *l(2)gl* to promote tumor-like overgrowth, this synergistic interaction being specifically and exclusively established only between *cno* and *scrib* loss in both systems (see Discussion).

DISCUSSION

In this work we have uncovered a synergistic interaction between *cno* and *scrib* mutants that leads to tumor-like overgrowth via Ras activation in both NBII lineages and epithelia. In NBII lineages, *cno scrib* mutant clones showed a much stronger phenotype than Ras^{V12} *scrib* clones. In the latter, the overexpression of Ras was able to overcome the JNK-mediated cell death in *scrib* NBII clones; however, Ras^{V12} *scrib* clones, despite displaying extra NBs, did not overgrow. This would suggest that the loss of *cno* in *cno scrib* clones has additional consequences other than activating Ras. Given that both *cno* and *scrib* modulate ACD, it is very plausible that the simultaneous loss of both regulators in NBII lineages contributes to exacerbating the phenotype by severely compromising this process. However, downregulating Ras signaling in *cno scrib* mutant clones suppressed their tumor-like overgrowth, strongly supporting the contention that both the upregulation of Ras activity and the accumulated ACD defects in *cno scrib* clones contribute to the tumor-like overgrowth phenotype. In epithelia, in antennal imaginal discs, both *cno scrib* and Ras^{V12} *scrib* clones showed upregulation of diP-MAPK and a concomitant overgrowth, although *cno scrib* clones to a lesser extent than Ras^{V12} *scrib* clones. The lower penetrance of the *cno scrib* phenotype is probably due to the much higher thresholds of Ras activity provided by Ras^{V12} (see also below). No apparent diP-MAPK upregulation or overgrowth was detected in *cno* or *scrib* single-mutant clones compared with control clones, indicating a synergism between these mutants also in imaginal discs.

Although the Raf–diP-MAPK signaling pathway was upregulated in response to Ras activation in imaginal discs, as previously shown (Brumby and Richardson, 2003), we were unable to detect diP-MAPK in NBII lineages in control or *cno scrib* clones, and it was at low levels or undetectable in Ras^{V12} clones. However, we found by different approaches that Ras is activated in *cno scrib* NBII clones, suggesting that other Ras effectors might be acting in those clones. Whereas in mammals Ras (K-, H- or N-Ras) can signal through different effectors, including Raf, PI3K and RALGDS, in *Drosophila* Ras acts mainly through the Raf-MAPK signaling cascade (Neuman-Silberberg et al., 1984). Interestingly, even though Ras does not normally act through PI3K in *Drosophila*, in wing imaginal discs Ras^{V12} is able to activate this pathway, which in turn leads to the activation of its downstream effector Akt1 (Prober and Edgar, 2002; Willecke et al., 2011). We have found that this scenario also occurs in *cno scrib* NBII clones, where the Ras-PI3K-Akt1 signaling pathway was aberrantly activated, and the overgrowth phenotype shown by these clones was suppressed by compromising this pathway.

Scrib functions along with Dlg1 and L(2)gl, forming part of what has been called the Scrib polarity module (Elsum et al., 2012). In fact, not only *scrib* but also *dlg1* and *l(2)gl* mutants cooperate with oncogenic Ras to induce tumor growth and metastasis in *Drosophila* imaginal discs (Brumby and Richardson, 2003; Igaki et al., 2006; Pagliarini et al., 2003). Hence, we examined whether *cno* loss would also synergistically interact with *dlg1* and *l(2)gl* to induce overgrowth. $dlg1^{RNAi}$ *cno* and $l(2)gl^{RNAi}$ *cno* double-mutant clones in antennal discs showed a marked overgrowth along with a clear upregulation of diP-MAPK. However, this phenotype was very similar to that shown by $dlg1^{RNAi}$ and $l(2)gl^{RNAi}$ single-mutant clones. This is intriguing because it suggests that both Dlg1 and L(2)gl are, directly or indirectly, impinging on the Ras-MAPK signaling pathway, promoting its repression. RAS is aberrantly activated in most human cancers. Hence, it is of great relevance to understand how it is normally regulated to avoid its oncogenic activity. To our knowledge, only Scrib, from the Scrib polarity module, has been described as inhibiting the Ras-MAPK pathway both in *Drosophila* and in mammalian cells by directly interacting with MAPK (Dow et al., 2008; Nagasaka et al., 2010). In zebrafish, *lgl(2)* (*llgl2*) loss has also been associated with an Erb-Ras signal upregulation (Reischauer et al., 2009). Altogether, we propose the existence of a coordinate and cooperative action in epithelial tissues between Cno and the Scrib/Dlg1/L(2)gl module to avoid aberrant Ras-MAPK signaling activation in normal conditions (Fig. 7T). The strongest effect on Ras-MAPK derepression found in both *dlg1* and *l(2)gl* single-mutant clones, as compared with *cno* and *scrib* single-mutant clones, might be due to the defects in Scrib localization or levels observed in the former mutants (Fig. 7G′,I′-J′). Given the high evolutionary conservation of these proteins, the cooperation between Cno and the Scrib module might also be functioning in humans (see below).

Like Scrib, Dlg1 and L(2)gl are also involved in regulating ACD in NBs. Thus, looking for potential synergisms between *cno* and *dlg1* or *l(2)gl* mutants in NBII lineages, we found that $dlg1^{RNAi}$ *cno* and $l(2)gl^{RNAi}$ *cno* double-mutant clones did not overgrow. In fact, they displayed defects characteristic of the *cno* single-mutant phenotype, such as the undersized NB. This indicates that *cno* is epistatic to both *dlg1* and *l(2)gl* during ACD in NBII lineages, which might explain the lack of synergisms between them.

Development (2017) 144, 2570-2583 doi:10.1242/dev.148171

Conversely, Cno and Scrib must function in parallel or in at least partially independent pathways during ACD in order to explain the strong synergism seen when both genes are compromised (Fig. 7T). Despite the extra NBs present in all *cno*, *l(2)gl*, *dlg1* and *scrib* NBII clones in the larval brain, the loss of each of these ACD regulators did not lead to a tumor-like overgrowth. On the contrary, these clones tended to be smaller and, in the case of *scrib* clones, they died by apoptosis. These observations might appear counterintuitive as *l(2)gl*, *dlg1* and *scrib* were originally identified as tumor suppressor genes due to the massive overgrowth they produced when they were compromised in the larval brain (Bilder et al., 2000; Gateff, 1994). It is important to remark, though, that these studies were not done by clonal NB analysis but in the homozygous mutant condition, and individual NB lineages were not analyzed in detail (NBII lineages had not even been described at that time). Contrary to what happens in homozygous mutant brains, NB mutant clones are surrounded by WT cells, which may counteract or even eliminate the clonal mutant cells, a phenomenon known as cell competition (Morata and Ballesteros-Arias, 2015). In the context of cancer biology, where tumors start with mutation(s) in one or a small group of cells, clonal analysis for studying the tumorigenic potential of particular gene mutations rather than analysis of the whole mutant tissue is a more disease-relevant scenario. In addition, an accepted hallmark in cancer biology is the acquisition of several mutational hits, not just single mutations, for tumor development (Hanahan and Weinberg, 2000, 2011), and our results support this. The differences in growth shown by *cno scrib* double-mutant clones (i.e. no overgrowth versus overgrowth, even massive overgrowth) might be due to the position of the mutant clone and differences in the environment or signals that could act to counteract or restrain mutant clone expansion.

The human afadin (*AFDN*, *MLLT4* or AF6 – for ALL1 fusion product on chromosome 6) gene was first isolated as a fusion partner of the mixed lineage leukemia gene (*MLL*, *ALL1* or *KMT2A*) that is frequently detected in acute lymphoblastic leukemias (Prasad et al., 1993). Recent work has established a direct connection between low levels of afadin and tumor growth in different cancer types (Fournier et al., 2011; Xu et al., 2015). Intriguingly, both Cno and afadin bind the activated form of Ras (Ras-GTP), *RAS* being one of the most commonly mutated oncogenes in human cancers, and we showed some years ago that Cno represses Ras during the specification of *Drosophila* muscle and heart progenitors (Carmena et al., 2006; Kuriyama et al., 1996). This inhibitory effect of Cno on Ras has been shown to be conserved in mammals (Fournier et al., 2011; Radziwill et al., 2003). Moreover, upregulation of Ras-GTP has recently been associated with afadin knockdown or to its translocation from the cytoplasm to the nucleus in distinct cancer types (Fournier et al., 2011; Manara et al., 2015). This is highly relevant because even though mutations in *RAS* alone do not normally progress in malignant tumors, they provide a sensitized genetic background for further mutational events, which along with mutated *RAS* can lead to neoplasias. This is the case with Ras^{V12} mutation, which causes aberrant Ras activation, and *scrib* tumor suppressor gene mutation, as mentioned above. In humans, SCRIB subcellular localization is altered or its levels are low in several cancer types, including breast cancer in which afadin is also downregulated with concomitant activation of the RAS-MAPK signaling pathway (Feigin et al., 2014; Fournier et al., 2011; Gardiol et al., 2006; Navarro et al., 2005; Zhan et al., 2008). Hence, the synergistic cooperation found in *Drosophila* between Cno and Scrib might be conserved between the human orthologs afadin and SCRIB.

MATERIALS AND METHODS

Drosophila strains and genetics

All stocks used were from the Bloomington Drosophila Stock Center and the Vienna Drosophila Resource Center, unless otherwise noted (see the supplementary Materials and Methods for a detailed description of strains). The crosses *GAL4×UAS* were carried out at 29°C. Balancer chromosomes bearing the *Tubby* dominant marker were used to identify third instar larva mutant chromosomes.

Generation of GFP-tagged endogenous *cno* gene lines

Intronic MIMIC insertions MI00782 (phase 1) and MI04707 (phase 0), containing two inverted ϕC31 attP target sites flanking a gene trap cassette, in the *cno* locus were replaced by pBS-KS-attB1-2-PT-SA-SD-1 or 0 (phase)-EGFP-FlAsH-StrepII-TEV-3xFlag using recombination-mediated cassette exchange (RMCE) (Venken et al., 2011).

MARCM clones

To generate mutant clones in the brain as well as in imaginal discs, *w; Dll-Gal4 UAS-CD8::GFP; FRT82B tubGal80* males or *hsFLP; Dll-Gal4 UAS-CD8::GFP; FRT82B tubGal80* females were crossed with females or males, respectively, of different genotypes (see the supplementary Materials and Methods for a detailed description of the crosses performed). The clones were identified by the presence of CD8::GFP. hsFLP was induced for 2 h at 37°C in late first/early second instar larvae and clones were analyzed in late third instar larvae.

Histology and immunofluorescence

Larval brains and discs were dissected and fixed in 3.7% formaldehyde in PBS for 40 min. Stainings were carried out using standard protocols. The following primary antibodies were used: mouse anti-Dlg1 1:100 (Developmental Studies Hybridoma Bank, DSHB), rabbit anti-Cnn 1:400 (a gift from T. C. Kaufman, Biology Indiana University, Bloomington, IN, USA), rabbit anti-PH3 1:400 (Millipore, 06-570), guinea pig anti-Dpn 1:200 (this work), rabbit anti-PntP1 1:500 (a gift from J. Skeath, Washington University School of Medicine, St Louis, MO, USA), rabbit anti-aPKCζ 1:100 (C-2 Santa Cruz, sc-216), rabbit anti-Baz 1:1000 (a gift from A. Wodarz, University of Cologne, CECAD Research Center, Cologne, Germany), rabbit anti-Pins 1:200 (a gift from J. Knoblich, Institute of Molecular Biotechnology, Vienna, Austria), guinea pig anti-Numb 1:400 [a gift from Y. N. Jan (Rhyu et al., 1994)], goat anti-Numb 1:200 (Santa Cruz, sc-23579), rabbit anti-Mira 1:1000 (Ikeshima-Kataoka et al., 1997), rabbit anti-Elav 1:400 (DSHB), rabbit anti-Ase 1:80 (this work), rabbit anti-L(2)gl 1:100 (Santa Cruz, sc-98260), mouse anti-diP-MAPK 1:500 (Sigma, M8159), mouse anti-GFP 1:100 (Roche, 11814460001) and rabbit anti-P-SAPK/JNK 1:200 (Cell Signaling, 4668). Secondary antibodies coupled to Alexa Fluor 488, 546 or 633 (Invitrogen) were used for immunofluorescence.

Generation of Dpn and Ase antibodies

An Ase peptide (CLSDESMIDAIDWWEAHAPKSNGACTNLSV) was used to immunize two New Zealand rabbits (Abyntek). *Dpn* was cloned in an expression vector after being PCR amplified from genomic DNA (a gift from J. Skeath). Dpn protein was expressed in *E. coli* and purified to immunize two guinea pigs (Abyntek).

Image acquisition, processing and data analysis

Fluorescence images were recorded using a Leica DM-SL upright microscope with spectral confocal acquisition software. All images were taken with an HCX Plan Apochromat 63×/1.32 or 40×/1.25 oil CS objective (Zeiss). Images were analyzed using ImageJ (Schindelin et al., 2015) and FIJI (Schindelin et al., 2012) and assembled from raw data using Adobe Photoshop. Statistical analyses were carried out with SPSS software (IBM) using Student's *t*-test. Graphical representation of *t*-tests employed simple bars or dispersion graphics.

Western blots

Six eye-antennal imaginal discs or ten brains from third instar larvae were dissected in PBS and homogenized for 30 min in lysis buffer [50 mM Tris pH 8.0, 150 mM NaCl, 0.1% SDS, 1 M EDTA, 1% Triton X-100, 1% sodium deoxycholate, protease inhibitors, 1 mM NaF, 100 mM Na_3VO_4, 2 mM PMSF and Complete Protease Inhibitor Cocktail (Roche) freshly added prior to use] on ice. Protein extracts were centrifuged at 5000 ***g*** at 4°C for 10 min. 5×Laemmli buffer with 0.1 M DTT was added to each sample, heated at 95°C for 10 min and centrifuged at maximum speed (8000 ***g***) for 2 min before being resolved by SDS-PAGE. From the whole-protein extract, material corresponding to one disc or five brains was loaded in each experiment. Spectra Multicolor High Range Protein Ladder (Fermentas) was used as a molecular weight marker. PVDF filters were immunoblotted with 1:1000 mouse anti-diP-MAPK/ERK1/2 (Sigma, M8159), 1:20,000 rabbit anti-MAPK (Sigma, M5670), 1:500 rabbit anti-pAkt (Ser473; Cell Signaling, 9271), 1:200 rabbit anti-pan Akt (Cell Signaling, 4691) or 1:5000 mouse anti-α-Tubulin (Sigma, T6199). Each experiment was repeated at least three times. Images were analyzed and quantified as above.

Acknowledgements

We thank G. Halder and H. Richardson, A. Wodarz, Y. N. Jan, J. Skeath, T. C. Kaufman, J. Knoblich, the Bloomington Drosophila Stock Center at the University of Indiana, the Vienna Drosophila Resource Center and the Developmental Studies Hybridoma Bank at the University of Iowa for kindly providing fly strains and reagents. We are grateful to S. Speicher for technical assistance.

Competing interests

The authors declare no competing or financial interests.

Author contributions

Conceptualization: A.C.; Validation: N.R.-Q.; Formal analysis: N.R.-Q., M.F., A.d.T.-J.; Investigation: N.R.-Q., M.F., A.d.T.-J.; Writing - original draft: A.C.; Writing - review & editing: A.C.; Visualization: N.R.-Q., A.C.; Supervision: A.C.; Project administration: A.C.; Funding acquisition: A.C.

Funding

N.R.-Q. was supported by a VALi+d contract from the Generalitat Valenciana; our laboratory was supported by Spanish Government (Ministerio de Economía y Competitividad, MINECO) grants BFU2012-33020, BFU2015-64251-P and by FEDER (European Regional Development Fund). The Instituto de Neurociencias in Alicante is a Center of Excellence Severo Ochoa.

Supplementary information

Supplementary information available online at
http://dev.biologists.org/lookup/doi/10.1242/dev.148171.supplemental

References

Albertson, R. and Doe, C. Q. (2003). Dlg, Scrib and Lgl regulate neuroblast cell size and mitotic spindle asymmetry. *Nat. Cell Biol.* **5**, 166-170.

Bello, B., Reichert, H. and Hirth, F. (2006). The brain tumor gene negatively regulates neural progenitor cell proliferation in the larval central brain of Drosophila. *Development* **133**, 2639-2648.

Bello, B. C., Izergina, N., Caussinus, E. and Reichert, H. (2008). Amplification of neural stem cell proliferation by intermediate progenitor cells in Drosophila brain development. *Neural Dev.* **3**, 5.

Betschinger, J., Mechtler, K. and Knoblich, J. A. (2006). Asymmetric segregation of the tumor suppressor brat regulates self-renewal in Drosophila neural stem cells. *Cell* **124**, 1241-1253.

Bilder, D., Li, M. and Perrimon, N. (2000). Cooperative regulation of cell polarity and growth by Drosophila tumor suppressors. *Science* **289**, 113-116.

Boone, J. Q. and Doe, C. Q. (2008). Identification of Drosophila type II neuroblast lineages containing transit amplifying ganglion mother cells. *Dev. Neurobiol.* **68**, 1185-1195.

Bowman, S. K., Rolland, V., Betschinger, J., Kinsey, K. A., Emery, G. and Knoblich, J. A. (2008). The tumor suppressors Brat and Numb regulate transit-amplifying neuroblast lineages in Drosophila. *Dev. Cell* **14**, 535-546.

Briggs, K. J., Corcoran-Schwartz, I. M., Zhang, W., Harcke, T., Devereux, W. L., Baylin, S. B., Eberhart, C. G. and Watkins, D. N. (2008). Cooperation between the Hic1 and Ptch1 tumor suppressors in medulloblastoma. *Genes Dev.* **22**, 770-785.

Brumby, A. M. and Richardson, H. E. (2003). scribble mutants cooperate with oncogenic Ras or Notch to cause neoplastic overgrowth in Drosophila. *EMBO J.* **22**, 5769-5779.

Carmena, A., Speicher, S. and Baylies, M. (2006). The PDZ protein Canoe/AF-6 links Ras-MAPK, Notch and Wingless/Wnt signaling pathways by directly interacting with Ras, Notch and Dishevelled. *PLoS ONE* **1**, e66.

Carmena, A., Makarova, A. and Speicher, S. (2011). The Rap1-Rgl-Ral signaling network regulates neuroblast cortical polarity and spindle orientation. *J. Cell Biol.* **195**, 553-562.

Caussinus, E. and Gonzalez, C. (2005). Induction of tumor growth by altered stem-cell asymmetric division in Drosophila melanogaster. *Nat. Genet.* **37**, 1125-1129.

Chen, G., Kong, J., Tucker-Burden, C., Anand, M., Rong, Y., Rahman, F., Moreno, C. S., Van Meir, E. G., Hadjipanayis, C. G. and Brat, D. J. (2014). Human Brat ortholog TRIM3 is a tumor suppressor that regulates asymmetric cell division in glioblastoma. *Cancer Res.* **74**, 4536-4548.

Cicalese, A., Bonizzi, G., Pasi, C. E., Faretta, M., Ronzoni, S., Giulini, B., Brisken, C., Minucci, S., Di Fiore, P. P. and Pelicci, P. G. (2009). The tumor suppressor p53 regulates polarity of self-renewing divisions in mammary stem cells. *Cell* **138**, 1083-1095.

Doe, C. Q. (2008). Neural stem cells: balancing self-renewal with differentiation. *Development* **135**, 1575-1587.

Dow, L. E., Elsum, I. A., King, C. L., Kinross, K. M., Richardson, H. E. and Humbert, P. O. (2008). Loss of human Scribble cooperates with H-Ras to promote cell invasion through deregulation of MAPK signalling. *Oncogene* **27**, 5988-6001.

Elsum, I., Yates, L., Humbert, P. O. and Richardson, H. E. (2012). The Scribble-Dlg-Lgl polarity module in development and cancer: from flies to man. *Essays Biochem.* **53**, 141-168.

Feigin, M. E., Akshinthala, S. D., Araki, K., Rosenberg, A. Z., Muthuswamy, L. B., Martin, B., Lehmann, B. D., Berman, H. K., Pietenpol, J. A., Cardiff, R. D. et al. (2014). Mislocalization of the cell polarity protein scribble promotes mammary tumorigenesis and is associated with basal breast cancer. *Cancer Res.* **74**, 3180-3194.

Fournier, G., Cabaud, O., Josselin, E., Chaix, A., Adelaide, J., Isnardon, D., Restouin, A., Castellano, R., Dubreuil, P., Chaffanet, M. et al. (2011). Loss of AF6/afadin, a marker of poor outcome in breast cancer, induces cell migration, invasiveness and tumor growth. *Oncogene* **30**, 3862-3874.

Gardiol, D., Zacchi, A., Petrera, F., Stanta, G. and Banks, L. (2006). Human discs large and scrib are localized at the same regions in colon mucosa and changes in their expression patterns are correlated with loss of tissue architecture during malignant progression. *Int. J. Cancer* **119**, 1285-1290.

Gateff, E. (1978). Malignant neoplasms of genetic origin in Drosophila melanogaster. *Science* **200**, 1448-1459.

Gateff, E. (1994). Tumor suppressor and overgrowth suppressor genes of Drosophila melanogaster: developmental aspects. *Int. J. Dev. Biol.* **38**, 565-590.

Gómez-López, S., Lerner, R. G. and Petritsch, C. (2014). Asymmetric cell division of stem and progenitor cells during homeostasis and cancer. *Cell. Mol. Life Sci.* **71**, 575-597.

Hanahan, D. and Weinberg, R. A. (2000). The hallmarks of cancer. *Cell* **100**, 57-70.

Hanahan, D. and Weinberg, R. A. (2011). Hallmarks of cancer: the next generation. *Cell* **144**, 646-674.

Hwang, W.-L., Jiang, J.-K., Yang, S.-H., Huang, T.-S., Lan, H.-Y., Teng, H.-W., Yang, C.-Y., Tsai, Y.-P., Lin, C.-H., Wang, H.-W. et al. (2014). MicroRNA-146a directs the symmetric division of Snail-dominant colorectal cancer stem cells. *Nat. Cell Biol.* **16**, 268-280.

Igaki, T., Pagliarini, R. A. and Xu, T. (2006). Loss of cell polarity drives tumor growth and invasion through JNK activation in Drosophila. *Curr. Biol.* **16**, 1139-1146.

Ikeshima-Kataoka, H., Skeath, J. B., Nabeshima, Y., Doe, C. Q. and Matsuzaki, F. (1997). Miranda directs Prospero to a daughter cell during Drosophila asymmetric divisions. *Nature* **390**, 625-629.

Ito, T., Kwon, H. Y., Zimdahl, B., Congdon, K. L., Blum, J., Lento, W. E., Zhao, C., Lagoo, A., Gerrard, G., Foroni, L. et al. (2010). Regulation of myeloid leukaemia by the cell-fate determinant Musashi. *Nature* **466**, 765-768.

Keder, A., Rives-Quinto, N., Aerne, B. L., Franco, M., Tapon, N. and Carmena, A. (2015). The hippo pathway core cassette regulates asymmetric cell division. *Curr. Biol.* **25**, 2739-2750.

Knoblich, J. A. (2008). Mechanisms of asymmetric stem cell division. *Cell* **132**, 583-597.

Kuriyama, M., Harada, N., Kuroda, S., Yamamoto, T., Nakafuku, M., Iwamatsu, A., Yamamoto, D., Prasad, R., Croce, C., Canaani, E. et al. (1996). Identification of AF-6 and canoe as putative targets for Ras. *J. Biol. Chem.* **271**, 607-610.

Land, H., Parada, L. F. and Weinberg, R. A. (1983). Tumorigenic conversion of primary embryo fibroblasts requires at least two cooperating oncogenes. *Nature* **304**, 596-602.

Lee, T., Lee, A. and Luo, L. (1999). Development of the Drosophila mushroom bodies: sequential generation of three distinct types of neurons from a neuroblast. *Development* **126**, 4065-4076.

Lee, C.-Y., Wilkinson, B. D., Siegrist, S. E., Wharton, R. P. and Doe, C. Q. (2006). Brat is a Miranda cargo protein that promotes neuronal differentiation and inhibits neuroblast self-renewal. *Dev. Cell* **10**, 441-449.

Liu, J. C., Voisin, V., Wang, S., Wang, D.-Y., Jones, R. A., Datti, A., Uehling, D., Al-awar, R., Egan, S. E., Bader, G. D. et al. (2014). Combined deletion of Pten and p53 in mammary epithelium accelerates triple-negative breast cancer with dependency on eEF2K. *EMBO Mol. Med.* **6**, 1542-1560.

Manara, E. Baron, E. Tregnago, C., Aveic, S., Bisio, V., Bresolin, S., Masetti, R., Locatelli, F., Basso, G. and Pigazzi, M. (2015). MLL-AF6 fusion oncogene sequesters AF6 into the nucleus to trigger RAS activation in myeloid leukemia. *Blood* **124**, 263-272.

Miyamoto, H., Nihonmatsu, I., Kondo, S., Ueda, R., Togashi, S., Hirata, K., Ikegami, Y. and Yamamoto, D. (1995). canoe encodes a novel protein containing a GLGF/DHR motif and functions with Notch and scabrous in common developmental pathways in Drosophila. *Genes Dev.* **9**, 612-625.

Morata, G. and Ballesteros-Arias, L. (2015). Cell competition, apoptosis and tumour development. *Int. J. Dev. Biol.* **59**, 79-86.

Nagasaka, K., Pim, D., Massimi, P., Thomas, M., Tomaic, V., Subbaiah, V. K., Kranjec, C., Nakagawa, S., Yano, T., Taketani, Y. et al. (2010). The cell polarity regulator hScrib controls ERK activation through a KIM site-dependent interaction. *Oncogene* **29**, 5311-5321.

Navarro, C., Nola, S., Audebert, S., Santoni, M.-J., Arsanto, J.-P., Ginestier, C., Marchetto, S., Jacquemier, J., Isnardon, D., Le Bivic, A. et al. (2005). Junctional recruitment of mammalian Scribble relies on E-cadherin engagement. *Oncogene* **24**, 4330-4339.

Neuman-Silberberg, F. S., Schejter, E., Hoffmann, F. M. and Shilo, B.-Z. (1984). The Drosophila ras oncogenes: structure and nucleotide sequence. *Cell* **37**, 1027-1033.

Ohshiro, T., Yagami, T., Zhang, C. and Matsuzaki, F. (2000). Role of cortical tumour-suppressor proteins in asymmetric division of Drosophila neuroblast. *Nature* **408**, 593-596.

Pagliarini, R. A., Quiñones, A. T. and Xu, T. (2003). Analyzing the function of tumor suppressor genes using a Drosophila model. *Methods Mol. Biol.* **223**, 349-382.

Parmentier, M. L., Woods, D., Greig, S., Phan, P. G., Radovic, A., Bryant, P. and O'Kane, C. J. (2000). Rapsynoid/partner of inscuteable controls asymmetric division of larval neuroblasts in Drosophila. *J. Neurosci.* **20**, RC84.

Peng, C.-Y., Manning, L., Albertson, R. and Doe, C. Q. (2000). The tumour-suppressor genes lgl and dlg regulate basal protein targeting in Drosophila neuroblasts. *Nature* **408**, 596-600.

Petronczki, M. and Knoblich, J. A. (2001). DmPAR-6 directs epithelial polarity and asymmetric cell division of neuroblasts in Drosophila. *Nat. Cell Biol.* **3**, 43-49.

Prasad, R., Gu, Y., Alder, H., Nakamura, T., Canaani, O., Saito, H., Huebner, K., Gale, R. P., Nowell, P. C., Kuriyama, K. et al. (1993). Cloning of the ALL-1 fusion partner, the AF-6 gene, involved in acute myeloid leukemias with the t(6;11) chromosome translocation. *Cancer Res.* **53**, 5624-5628.

Prober, D. A. and Edgar, B. A. (2002). Interactions between Ras1, dMyc, and dPI3K signaling in the developing Drosophila wing. *Genes Dev.* **16**, 2286-2299.

Radziwill, G., Erdmann, R. A., Margelisch, U. and Moelling, K. (2003). The Bcr kinase downregulates Ras signaling by phosphorylating AF-6 and binding to its PDZ domain. *Mol. Cell. Biol.* **23**, 4663-4672.

Reischauer, S., Levesque, M. P., Nüsslein-Volhard, C. and Sonawane, M. (2009). Lgl2 executes its function as a tumor suppressor by regulating ErbB signaling in the zebrafish epidermis. *PLoS Genet.* **5**, e1000720.

Rhyu, M. S., Jan, L. Y. and Jan, Y. N. (1994). Asymmetric distribution of numb protein during division of the sensory organ precursor cell confers distinct fates to daughter cells. *Cell* **76**, 477-491.

Schindelin, J., Arganda-Carreras, I., Frise, E., Kaynig, V., Longair, M., Pietzsch, T., Preibisch, S., Rueden, C., Saalfeld, S., Schmid, B. et al. (2012). Fiji: an open-source platform for biological-image analysis. *Nat. Methods* **9**, 676-682.

Schindelin, J., Rueden, C. T., Hiner, M. C. and Eliceiri, K. W. (2015). The ImageJ ecosystem: An open platform for biomedical image analysis. *Mol. Reprod. Dev.* **82**, 518-529.

Schober, M., Schaefer, M. and Knoblich, J. A. (1999). Bazooka recruits Inscuteable to orient asymmetric cell divisions in Drosophila neuroblasts. *Nature* **402**, 548-551.

Speicher, S., Fischer, A., Knoblich, J. and Carmena, A. (2008). The PDZ protein Canoe regulates the asymmetric division of Drosophila neuroblasts and muscle progenitors. *Curr. Biol.* **18**, 831-837.

Sugiarto, S., Persson, A. I., Munoz, E. G., Waldhuber, M., Lamagna, C., Andor, N., Hanecker, P., Ayers-Ringler, J., Phillips, J., Siu, J. et al. (2011). Asymmetry-defective oligodendrocyte progenitors are glioma precursors. *Cancer Cell* **20**, 328-340.

Venken, K. J., Schulze, K. L., Haelterman, N. A., Pan, H., He, Y., Evans-Holm, M., Carlson, J. W., Levis, R. W., Spradling, A. C., Hoskins, R. A. et al. (2011). MiMIC: a highly versatile transposon insertion resource for engineering Drosophila melanogaster genes. *Nat. Methods* **8**, 737-743.

Willecke, M., Toggweiler, J. and Basler, K. (2011). Loss of PI3K blocks cell-cycle progression in a Drosophila tumor model. *Oncogene* **30**, 4067-4074.

Wodarz, A., Ramrath, A., Kuchinke, U. and Knust, E. (1999). Bazooka provides an apical cue for Inscuteable localization in Drosophila neuroblasts. *Nature* **402**, 544-547.

Wodarz, A., Ramrath, A., Grimm, A. and Knust, E. (2000). Drosophila atypical protein kinase C associates with Bazooka and controls polarity of epithelia and neuroblasts. *J. Cell Biol.* **150**, 1361-1374.

Wu, M., Kwon, H. Y., Rattis, F., Blum, J., Zhao, C., Ashkenazi, R., Jackson, T. L., Gaiano, N., Oliver, T. and Reya, T. (2007). Imaging hematopoietic precursor division in real time. *Cell Stem Cell* **1**, 541-554.

Xu, Y., Chang, R., Peng, Z., Wang, Y., Ji, W., Guo, J., Song, L., Dai, C., Wei, W., Wu, Y. et al. (2015). Loss of polarity protein AF6 promotes pancreatic cancer metastasis by inducing Snail expression. *Nat. Commun.* **6**, 7184.

Yu, F., Cai, Y., Kaushik, R., Yang, X. and Chia, W. (2003). Distinct roles of Galphai and Gbeta13F subunits of the heterotrimeric G protein complex in the mediation of Drosophila neuroblast asymmetric divisions. *J. Cell Biol.* **162**, 623-633.

Zhan, L., Rosenberg, A., Bergami, K. C., Yu, M., Xuan, Z., Jaffe, A. B., Allred, C. and Muthuswamy, S. K. (2008). Deregulation of scribble promotes mammary tumorigenesis and reveals a role for cell polarity in carcinoma. *Cell* **135**, 865-878.